Desalination and Water Treatment
www.deswater.com
doi: 10.1080/19443994.2013.867816

53 (2015) 2636–2644
March

Taylor & Francis
Taylor & Francis Group

Synthesis and characterization of functionalized polyacrylonitrile coated with iron oxide nanoparticles and its applicability in nitrate removal from aqueous solution

Ramin Nabizadeh[a,b], Mahsa Jahangiri-Rad[c,*], Masoud Yunesian[a,b], Jafar Nouri[c], Faramarz Moattar[c], Sodeh Sadjadi[d]

[a]*Center for Water Quality Research, Institute for Environmental Research, Tehran University of Medical Sciences, Tehran, Iran*
[b]*Department of Environmental Health Engineering, School of Public Health, Tehran University of Medical Sciences, Tehran, Iran*
[c]*Department of Environmental Sciences, Graduate School of the Environment and Energy, Tehran Science and Research Branch, Islamic Azad University, Tehran, Iran*
Tel. +9821 4486 9443; email: mahsajahangiri_64@yahoo.com
[d]*Nuclear Science and Technology Research Institute, Nuclear fuel cycle school, Tehran, Iran*

Received 4 April 2013; Accepted 12 November 2013

ABSTRACT

A novel adsorbent, Polyacrylonitrile (PAN)-oxime-nano-Fe_2O_3, was developed to remove nitrates from water. The properties of the adsorbent were characterized by transmission electron microscopy, X-ray diffraction, and Fourier transform infrared spectroscopy. Experiments were carried out to investigate the adsorption kinetics and desorption behaviour of the adsorbent. The Langmuir, Freundlich, and Dubinin–Radushkevich (D–R) isotherms were determined and the results revealed that the adsorption was well explained by the (D–R) model. The experimental data fitted very well the pseudo-second-order kinetic model. Intra-particle diffusion affects nitrate uptake. The experiments showed that the maximum amount of nitrate released after desorption processes was about 50%, indicating that a large portion of nitrate was irreversibly retained by the PAN-oxime-nano-Fe_2O_3.

Keywords: Polyacrylonitrile; Nano-Fe_2O_3; Adsorption isotherms; Kinetics

1. Introduction

The treatment and disposal of nitrate-contaminated water has become one of the most serious environmental problems worldwide over the past few decades. The principle sources of nitrate in water are run-off and drainage from land treated with agricultural fertilizers and also deposition from the atmosphere as a consequence of NO_x released from fossil fuel combustion [1]. The nitrogen existing in organic soil medium may also be released as nitrate through microbial activities [2]. Nitrate pollution of some surface and ground waters has been a major problem in some agricultural areas [3]. Nitrate's role as a nutrient contributes predominately to blooms of algae, which subsequent to their decomposition deprive water of oxygen [1,2]. There has long been concern expressed over the existence of nitrate in drinking water at concentrations exceeding the US Environmental

*Corresponding author.

Protection Agency guideline of 50 mg L^{-1} (10 mg L^{-1} as NO_3–N) due to the risk of methaemoglobinaemia. The association constant for methaemoglobin formation is larger than that for formation of the oxyhemoglobin complex. Thus, nitrate ions bind with haemoglobin, depriving tissues of oxygen. Severe cases of this disease can result in mental retardation in infants and even death from asphyxiation. At stomach pH, nitrate is also converted to $H_2NO_2^+$, which is capable of nitrosating secondary amines and secondary amides. The resulting N-nitrosamines may be carcinogenic [4]. Due to regulation worldwide, nitrate should be removed from potable water. The most commonly used treatment methods to remove/reduce NO_3^- include chemical denitrification using zero-valent iron (Fe^0) [5,6], zero-valent magnesium [7], ion exchange (IX) [8], reverse osmosis [9], electrodialysis [10], catalytic denitrification [11], biological denitrification [12], and adsorption [13]. Among the different treatments described above, adsorption technology with no chemical degradation is attractive due to its efficiency and economy. Adsorption technology has been considered successful in removing different types of inorganic anions, e.g. fluoride [14], nitrate [15], and bromate [16] from waters using various adsorbents. Polyacrylonitrile (PAN) and its copolymers have been widely studied for commercial/technological exploitation. Cross-linking of PAN can impart some of its important physical properties, such as insolubility and resistance to swelling in common solvents [17,18]. The high crystalline melting point (317˚C) of PAN and its limited solubility in certain solvents is due to the intermolecular forces between the polymer chains [19]. Active nitrile groups present in PAN copolymers allow the introduction of new functional groups by special reactions. Researchers have reported various methods of PAN modification to obtain cationite, anionite, and ampholyte derivatives [20]. Zero-valent iron (ZVI) has been studied for its ability to reduce different contaminants including nitrate in groundwater [5,21]. However, this technology has several drawbacks, including ammonium production and also requirement for pH control [5]. Nitrate removal by different adsorbents has been studied using nano sized particles. In recent years, nanotechnology has emerged as one of the attractive technologies for water treatment. The benefits of using nano materials derive from their large surface areas and properties of self-assembly and enhanced reactivity; therefore, they can be applied to water treatment [22]. In this work, PAN-oxime was synthesized through modification of PAN, and the modified PAN was coated with iron oxide nanoparticles (Fe_2O_3). The PAN-oxime-nano-Fe_2O_3 was subsequently used for the adsorption of nitrate.

2. Experimental

2.1. Materials

Sodium carbonate, hydroxylamine hydrochloride, and sodium nitrate were purchased from the Merck Company. A nitrate stock solution was prepared by dissolving sodium nitrate in deionized (DI) water and stored in the dark at 4˚C. Standards and nitrate-spiked samples in the required concentration range were prepared by appropriate dilution of the stock solution with DI water. All reagents used were of analytical reagent grade.

2.2. Preparation of Fe_2O_3

The Fe_2O_3 nano particles were prepared by a previously described method. In a typical procedure, 0.025 M citric acid, 0.005 M $FeSO_4{\cdot}7H_2O$, and 1.2 g of polyethylene glycol (PEG)-6000 were added to 50 mL of distilled water and ethanol (in a volume ratio of 3:2) with vigorous stirring. The mixture turned yellow, and was then evaporated at 85˚C for 5 h, by which point it had turned into a polymeric gel (resin). The obtained resin was dried at 135˚C for 5 h and a dry gel was obtained. The resulting materials were calcined at 600˚C for 5 h to obtain the Fe_2O_3 nano powder [23].

2.3. Functionalization of PAN

Fig. 1 represents the reaction of hydroxylamine hydrochloride with the PAN nitrile group. Hydroxylamine hydrochloride (16 g), sodium carbonate (12 g), and 0.4 g of PAN powder were added to a 250 mL bottle to which 100 mL of DI water was added and shaken. The reaction was carried out at 70˚C for 120 min. After reaction, the mixture was filtered and left to dry. The PAN was functionalized with a Fe_2O_3 coating by adding 0.2 g of the prepared Fe_2O_3 nano powder, functionalized PAN, and 100 mL DI water to a sealed bottle. The solution was shaken at 70˚C for 120 min. The resulting mixture was filtered and dried in a vacuum oven at 60˚C [24]. The PAN functionalized Fe_2O_3 was then used as an adsorbent.

2.4. Characterization of the adsorbent

The functional groups and iron oxide nano particles on the PAN were detected on a Fourier transform infrared (FT-IR) spectrometer. X-ray diffraction (XRD) measurements of the catalyst powder were recorded using a Philips PW 1800 diffractometer. The FT-IR spectra of the samples were recorded on a FT-IR Brucker Tensor 27 spectrometer. The particle size and

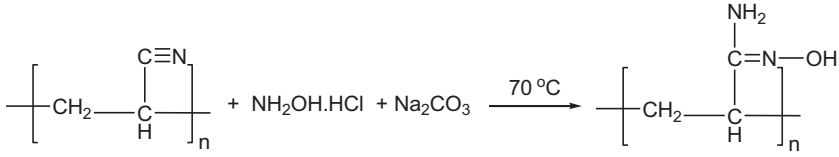

Fig. 1. Functionalization of PAN with hydroxylamine hydrochloride.

morphology of the nano crystalline particle were examined using a transmission electron microscope (TEM) (LEO 912AB). The BET surface area was determined from adsorption isotherm using a micrometrics surface area analyzer (ASAP 2020).

2.5. Batch adsorption experiments

Batch adsorption experiments were conducted using 100 mL glass bottles with the addition of 30 mg of adsorbents and 50 mL of nitrate solutions of increasing initial concentration (C_0) from 20 to 200 mg L^{-1}. The nitrate concentration range was chosen to be representative of nitrate levels in some ground water bodies. The solutions were shaken in an illuminated refrigerated incubator shaker (Innova 4340) at ambient temperature (25 ± 2°C). After equilibrating, the solid was separated by centrifugation (3,000 rpm) and filtration (0.22 μ). The filtrates were then analyzed spectrophotometrically. This method is based on instructions of *standard methods for the examination of water and wastewater* (part 4500-NO_3). In the experiments on the effect of temperature, the temperature was held at 298, 303, and 308°C. At the end of equilibrium period, the suspensions were separated for later analysis of the nitrate concentration. The reproducibility of the measurements was determined from triplicates and average values are reported. The amount of nitrate adsorbed (q_e in mg g^{-1}) was calculated as follows:

$$q_e = (C_0\text{-}C_e)V/m \quad (1)$$

where C_0 and C_e are the initial and equilibrium concentrations of nitrate in solution (mg/L), respectively, V is the volume of the solution and m is the mass of the adsorbent (g).

2.6. Kinetic studies

The rate of adsorption of nitrate was studied at different time intervals (1–24 h). In kinetic studies, 50 mL of nitrate solution (100 mg L^{-1}) was agitated with functionalized-PAN-Fe_2O_3 nano particles (0.03 g). At fixed time intervals, the adsorbent was separated and the filtrate was analyzed to determine the equilibrium concentration of nitrate. Experiments were repeated for different periods until the adsorption equilibrium was reached.

2.7. Desorption studies

The reversibility of nitrate adsorption on the PAN-oxime-nano-Fe_2O_3 was determined by performing desorption experiments as already described. Once equilibrium was reached, the adsorbent was removed from the nitrate solution, washed with DI water, and placed inside a bottle containing 50 mL of a desorbing solution (DI water) without nitrate. The aim of the washing step was to remove any nitrate solution trapped in pores of the PAN-oxime-nano-Fe_2O_3. The saturated PAN-oxime-nano-Fe_2O_3 and the desorbing solution were shaken for 24 h until they reached a new equilibrium. The mass of nitrate that remained adsorbed on the PAN-oxime-nano-Fe_2O_3 was calculated with a mass balance.

3. Results and discussion

3.1. Characterization of PAN-oxime-nano-Fe_2O_3

Fig. 2 shows the FT-IR spectra of PAN, functionatized PAN, and the XRD pattern of functionalized PAN-Fe_2O_3 nano particles. The FT-IR spectrum of PAN (Fig. 2(a)) exhibited the characteristic bands of nitrile (2,238 cm^{-1}), carbonyl (1,728 cm^{-1}), and ether (1,229 and 1,070 cm^{-1}) groups; the carbonyl and ether bands came from the methylacrylate co-monomer. The FT-IR spectrum of the functionalized PAN (Fig. 2(b)) showed all the characteristic bands of the functional groups on PAN, with additional peaks at 910 and 1,662 cm^{-1} due to the stretching vibrations of N–O and C=N groups in the functionalized PAN, respectively [25]. Furthermore, the intensity of the nitrile peak of the functionalized PAN decreased. All these changes confirm the introduction of oxime groups on the PAN. The XRD patterns of the Fe_2O_3

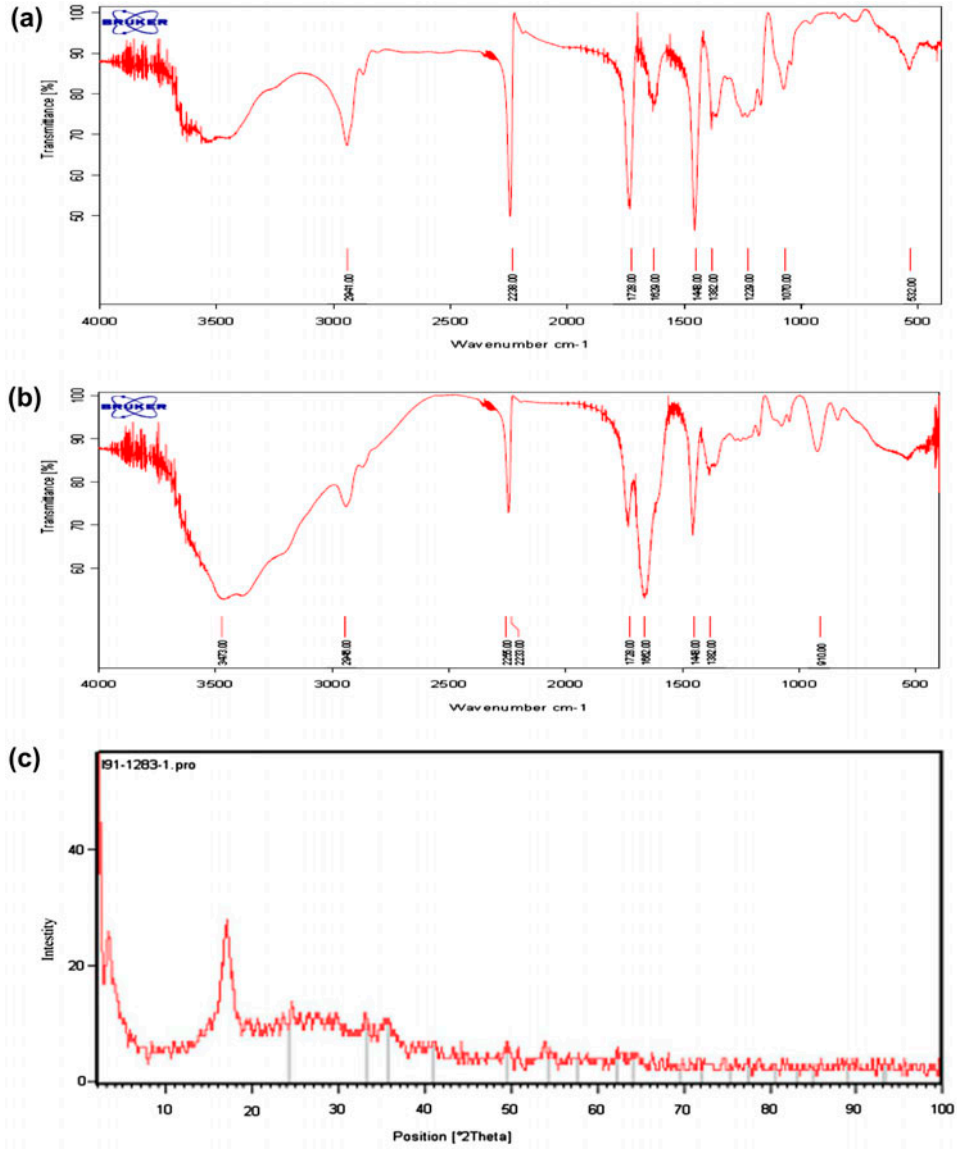

Fig. 2. (a) FT-IR pattern of PAN, (b) functionalized PAN, and (c) XRD pattern of oxime-nano-Fe_2O_3.

nano particles and functionalized PAN-Fe_2O_3 are shown in Fig. 2(c). The XRD patterns of functionalized PAN-Fe_2O_3 show a broad non-crystalline peak (2θ = 20°–30°) and a crystalline peak (2θ = 18°) corresponding to the orthorhombic PAN (110) reflection; in addition to the diffraction peaks of the PAN phase, other peaks appeared corresponding to the Fe_2O_3, indicating that the Fe_2O_3 nano particles on the PAN have the same crystal diffraction as pure Fe_2O_3.The morphologies of the adsorbent are characterized by TEM. As shown in Fig. 3, Fe_2O_3 nano particles are attached to the surface of functionalized PAN. The BET surface area and pore volume was 155 $m^2\ g^{-1}$ and 0.95 $cm^3\ g^{-1}$, respectively.

3.2. *Adsorption isotherms*

The adsorption equilibrium isotherm is important for describing how the adsorbate molecules distribute between the liquid and solid phases. The adsorption isotherm of nitrate on PAN-oxime-nano-Fe_2O_3 is shown in Fig. 4. As shown in Fig. 4, the equilibrium uptake increased with increasing equilibrium nitrate concentration over the experimental concentration range. A maximum experimental adsorption capacity of 24.4 $mg\ g^{-1}$ was observed for nitrate on PAN-oxime-nano-Fe_2O_3 at 25 ± 2°C; whereas, the theoretical adsorption capacity based on Dubinin–Radushkevich (D–R) isotherm model was obtained as 18.41 $mg\ g^{-1}$.

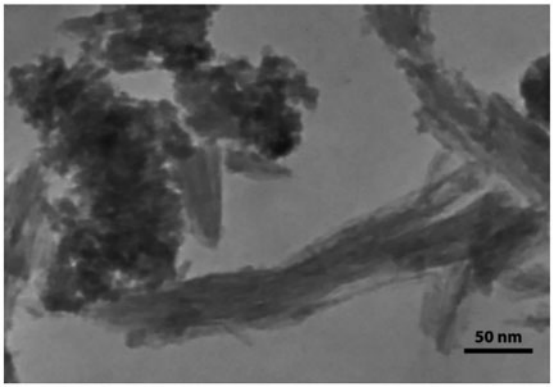

Fig. 3. TEM image of functionalized PAN-Fe_2O_3.

The initial sharp rise in the isotherm indicates the

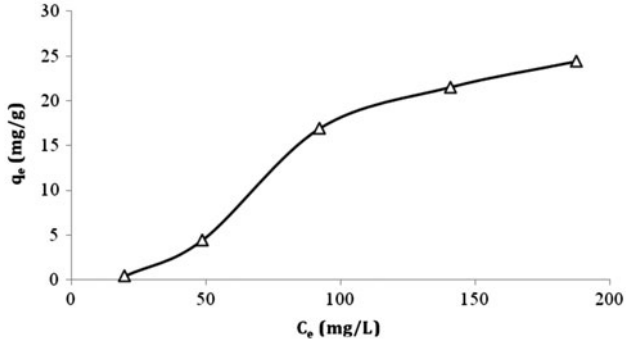

Fig. 4. Adsorption isotherm of nitrate onto PAN-oxime-nano-Fe_2O_3.

availability of readily accessible sites for adsorption. However, as the nitrate concentration increases a plateau is reached, indicating virtually no more sites remain available for further adsorption. The initial concentration provides an important driving to overcome all mass transfer resistances of the nitrate between the aqueous and solid phases [26].

The concentration of the equilibrium data with either theoretical or empirical equations is essential to practical operations. The isotherm data were fitted to the Langmuir and Freundlich isotherms. The Langmuir isotherm assumes that the free energy of adsorption does not depend on the surface coverage. It also predicts the saturation of the solid surface, with monolayer coverage by the adsorbate at high C_e and linear adsorption at low C_e values [27]. This model is represented by the following linear equation [28]:

$$\frac{1}{q_e} = \frac{1}{q_m} + \frac{1}{q_m b C_e} \quad (2)$$

where C_e (mg L^{-1}) is the equilibrium concentration, q_e (mg g^{-1}) is the amount of adsorbate adsorbed per unit mass of adsorbate, and q_m and b are the Langmuir constants related to adsorption capacity and rate of adsorption, respectively. When $1/q_e$ was plotted against $1/c_e$, a straight line with slope $1/q_m$ b was obtained (Fig. 5(a)). The Langmuir constants were calculated from this isotherm and their values are listed in Table 1. Another important parameter, R_L, the separation factor or equilibrium parameter is determined from the relation:

$$R_L = 1/1 + bC_0 \quad (3)$$

where b is the Langmuir Constant and C_0 (mg L^{-1}) is the highest nitrate concentration. The value of R_L shows this type of isotherm to be either favourable ($0 < R_L < 1$) or unfavourable ($R_L > 1$), linear ($R_L = 1$), or irreversible ($R_L = 0$) [29]. The R_L values for the maximum and minimum nitrate concentration in the present study are 0.367 and 0.0367, respectively, which confirms that adsorption of nitrate by this material is favorable under the conditions of this research.

The Freundlich isotherm model is an empirical relationship, which assumes that the ratio of the

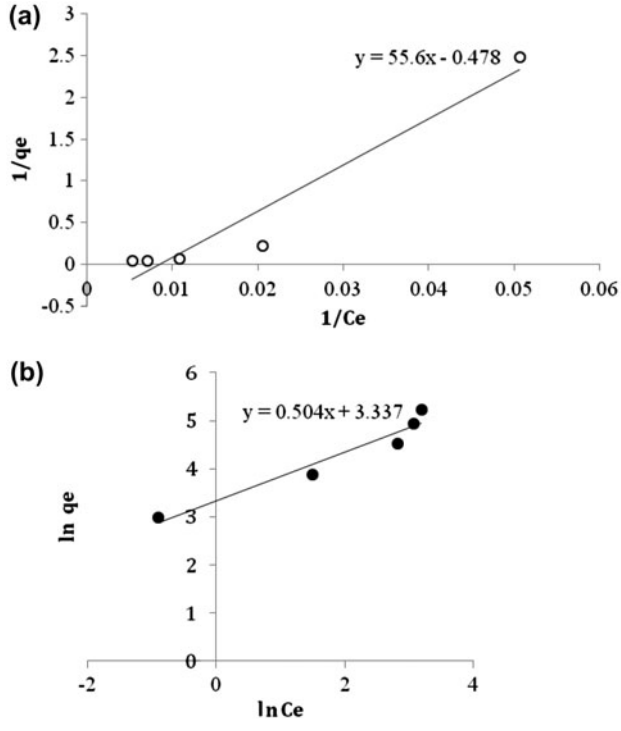

Fig. 5. (a) Langmuir and (b) Freundlich isotherms for nitrate adsorption onto PAN-oxime-nano-Fe_2O_3.

Table 1
Constant of Freundlich, Langmuir, and D–R isotherms of nitrate

Langmuir model: $\frac{1}{q_e} = \frac{55.6}{C_e} - 0.478$		
q_m (mg g^{-1})	b (L mg^{-1})	R^2
2.09	0.0086	0.938
Freundlich model: Ln q_e = 0.504 Ln C_e + 3.337		
K_f ((mg g^{-1})(L mg^{-1})$^{1/n}$)	n	R^2
16.17	1.98	0.936
Dubinin–Radushkevich (D–R) isotherm: Ln q_e = Ln q_m − $\beta\varepsilon^2$		
q_m	β	R^2
18.41	0.0001	0.955

amount of solute adsorbed onto a given mass of adsorbate to the concentration of the solute in solution is not constant at different solution concentrations. In other words, different sites with distinct adsorption energies are involved. The linear form of the Freundlich equation is [30]:

$$\text{Ln}\, q_e = \text{Ln}\, k_f + 1/n\, \text{Ln}\, C_e \quad (4)$$

where q_e is the amount of nitrate adsorbed at equilibrium mg g^{-1} and C_e is the equilibrium concentration. K_f and n are Freundlich constants. The plot of Ln q_e vs. Ln C_e is shown in Fig. 5(b). The Langmuir and Freundlich constants were calculated and are listed in Table 1.

It has been reported that values of n in the 2–10 range represent good, 1–2 moderately difficult, and <1 poor adsorption characteristics. In the present research, the n obtained was 1.98, indicating that the adsorption is moderately difficult.

The nature of the adsorption (physical or chemical) was also analyzed with the D–R isotherm [31]. The linear form of the D–R isotherm equation can be expressed as:

$$\text{Ln}\, q_e = \text{Ln}\, q_m\text{-}B\varepsilon^2 \quad (5)$$

where q_e is the amount of nitrate adsorbed per unit mass of adsorbent (mg g^{-1}), q_m is the theoretical adsorption capacity, B is the constant of the sorption energy in relation to the average energy of sorption per mole of adsorbate [30], and ε is the Polanyi potential which is shown as:

$$\varepsilon = RT\, \text{Ln}(1 + 1/C_e) \quad (6)$$

where T is the temperature (K) and R is the gas constant. The value of mean sorption energy is calculated from:

$$E = 1/\sqrt{-2\beta} \quad (7)$$

The value of E is of great importance in anticipating the type of adsorption. If the value is below 8 kJ mol^{-1} then the adsorption is physical, if it is more than 8 kJ mol^{-1} then the adsorption is chemical in nature [31]. Fig. 6 shows the plot of q_e vs. ε^2; the value of E in this research was 0.08 kJ mol^{-1}, suggesting the physical nature of the adsorption.

3.3. Kinetic analysis

The effect of contact time on nitrate adsorption (100 mg L^{-1}) is shown in Fig. 7. The quantity of adsorbed solute (mg g^{-1}) increased with increasing time of contact and reached equilibrium after 45 min. To elucidate the adsorption kinetic process, the results from the kinetic analysis were modeled using pseudo-first-order and pseudo-second-order kinetic models [32]. The values obtained from intra-particle diffusion model (Table 2) were found to be in good agreement with the data and can be used to favorably explain the nitrate sorption. The rate equation and the related values are shown in Table 2. The kinetic plots generated by pseudo-first-order and pseudo-second-order

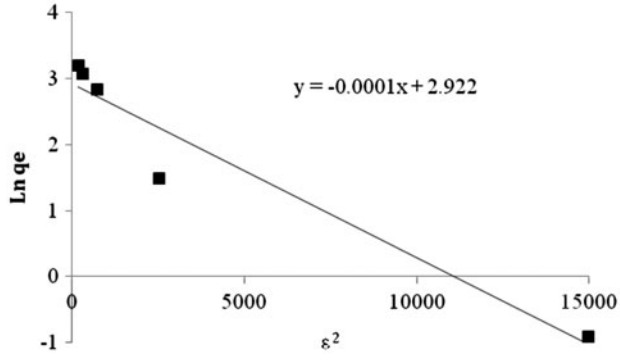

Fig. 6. D–R isotherm of nitrate onto PAN-oxime-nano-Fe_2O_3.

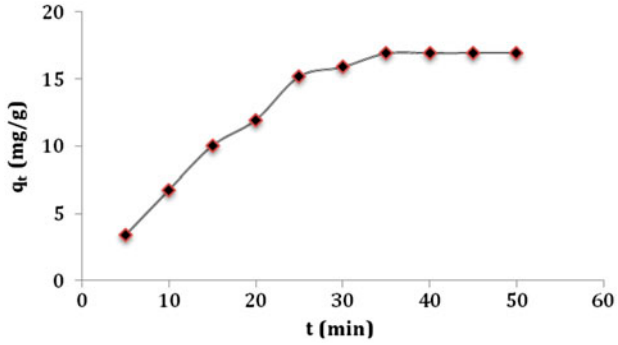

Fig. 7. Effect of contact time on fluoride adsorption on PAN-oxime-nano-Fe_2O_3.

Table 2
Pseudo-first and second-order and intra-particle diffusion model parameters

Pseudo-first-order model: Ln $(q_e - q_t) = -0.199t + 4.658$		
q_e (mg g^{-1})	K_1 (L min^{-1})	R^2
49.51	0.199	0.856
Pseudo-second-order model: $t/q_t = 0.033t + 0.158$		
q_e (mg g^{-1})	K_2 (g mg^{-1} min^{-1})	R^2
30.3	0.001	0.953
Intra-particle diffusion model: $q_t = 3.244\ t^{1/2} + 2.899$		
k_i (mg g^{-1} $min^{-0.5}$)	C (mg g^{-1})	R^2
3.244	2.899	0.947

kinetic models along with the experimental kinetic plot are given in Fig. 8. It can be seen from Table 2 that data showed an agreement with pseudo-second-order model (R^2 = 0.95). Hence, the pseudo-second-order model better represents the sorption kinetics.

Since, neither the pseudo-first-order nor the second-order models can identify the diffusion mechanism, the kinetic results were analyzed using an intra-particle diffusion model, which is expressed as [33]:

$$q_t = k_i t^{1/2} + c \tag{8}$$

where c is the intercept and k_i is the intra-particle diffusion rate constant (mg g^{-1} $min^{1/2}$). The equation and value of k_i are given in Table 2. Fig. 8(c) shows the intra-particle diffusion regression model. Typically, various mechanisms control adsorption kinetics; the most limiting are external diffusion, the boundary layer and intra-particle diffusion [34].

when the line of q_t vs. $t^{1/2}$ passes through the origin (C = 0), intra-particle diffusion will be the sole rate-controlling step. If the plot does not pass through the origin it shows that intra-particle diffusion is not the only rate-controlling step and other processes may control the rate of sorption [34].

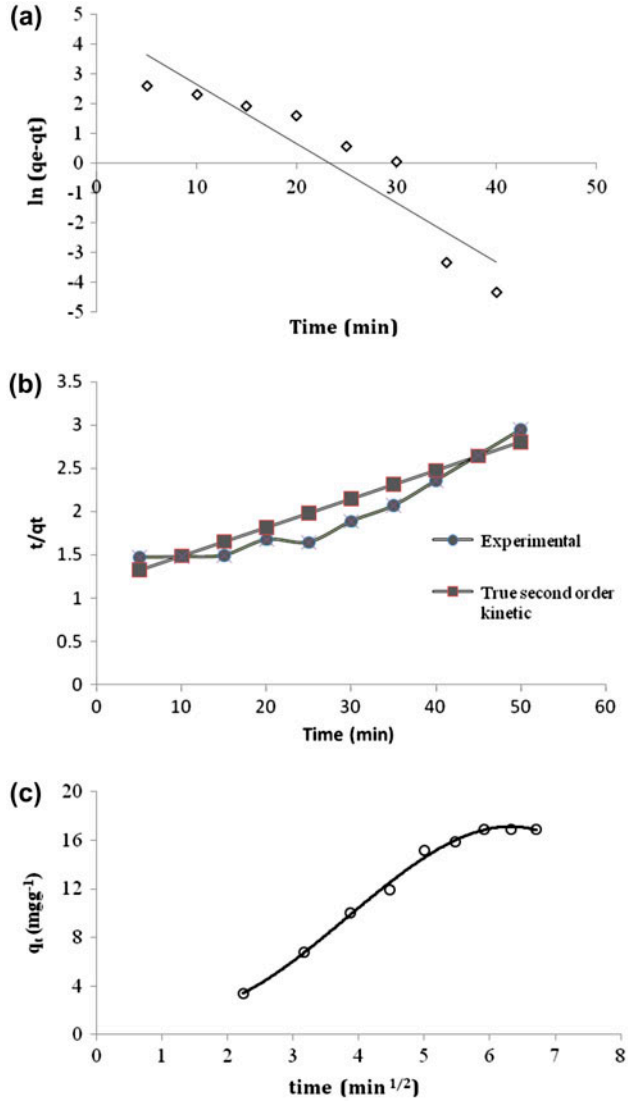

Fig. 8. Plots of (a) pseudo-first-order model, (b) pseudo-second-order model and (c) intra-particle diffusion model.

The results show that the intra-particle diffusion step was involved in the removal process (R^2 = 0.947) but was not the only rate control step (C ≠ 0). As can be seen from Fig. 8(c), nitrate sorption involves two stages, that is, surface sorption and intra-particle diffusion. The first linear portion is attributed to the boundary layer diffusion effect and the final linear portion may be due to the intra-particle diffusion effect.

3.4. Reversibility of the adsorption of nitrate on PAN-oxime-nano-Fe_2O_3

The reversibility of the nitrate adsorption was studied by conducting adsorption-desorption experiments. If the desorption equilibrium data fell on the

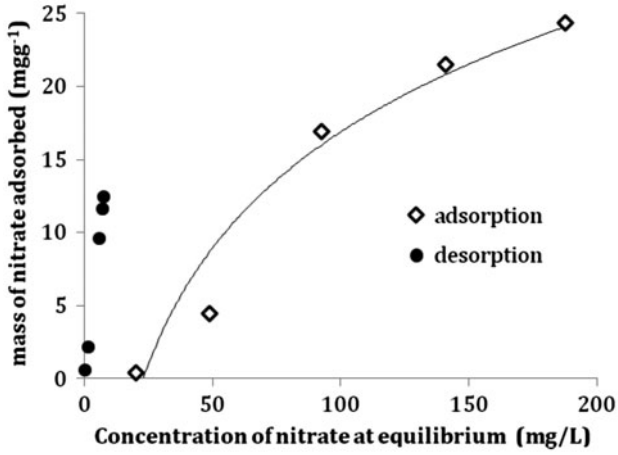

Fig. 9. Adsorption and desorption isotherms of nitrate on the PAN-oxime-nano-Fe_2O_3.

adsorption isotherm, the adsorption would be irreversible. The experimental data on adsorption–desorption of nitrate on the adsorbent as well as the adsorption isotherm are shown in Fig. 9. It can be observed from Fig. 9 that the desorption data plotted above the adsorption isotherm, thus the nitrate absorption was not completely reversible. However, the amount of nitrate desorbed was augmented as the concentration of nitrate adsorbed on PAN-oxime-nano-Fe_2O_3 was increased from previous steps.

4. Conclusion

(1) Nitrate sorption on PAN-oxime-nano-Fe_2O_3 was studied in batch mode and found to be strongly dependent on initial nitrate concentration.
(2) Nitrate sorption isotherm data were fitted well D–R isotherm and the maximum sorption capacity was found to be 24.4 mg g^{-1}. The n obtained was 1.98, indicating the adsorption is moderately difficult. *E* value (0.08 kJ mol^{-1}) from D–R model indicates that the type of sorption of nitrate on PAN-oxime-nano-Fe_2O_3 is physical.
(3) The pseudo-second-order kinetic model agrees very well the dynamic data for nitrate sorption on. Intra-particle diffusion affects nitrate uptake.
(4) The desorption capacity of nitrate from PAN-oxime-nano-Fe_2O_3 increased as initial nitrate concentration increased. At the maximum concentration only 25% of nitrate was desorbed, indicating that PAN-oxime-nano-Fe_2O_3 is not recyclable for further adsorption of nitrate.

Acknowledgments

This research was supported by Institute for Environmental Research, Tehran University of Medical sciences and technical laboratory support of KimiaFaam Pharmaceutical Company.

References

[1] A.E. Bailey-Watts, I.M.D. Gunn, A. Kirika, Loch Leven: Past and Current Water Quality and Options for Change, Report to the Fourth River Purification Board, Institute of Freshwater Ecology, Edinburgh, 1993.
[2] G.S. Douglas, A.E. Bence, R.C. Prince, S.J. McMillen, E.L. Butler, Environmental stability of selected petroleum hydrocarbon source and weathering ratios, Environ. Sci. Technol. 30 (1996) 23–32.
[3] E. Manahan Stanley, Fundamentals of Environmental Chemistry, Taylor & Francis, Colombia, 2001.
[4] N.B. Vladimir, Environmental Chemistry: Asian Lessons, Kluwer Academic Publishers, New York, NY, 2003.
[5] I.F. Cheng, R. Muftikian, Q. Fernando, N. Korte, Reduction of nitrate to ammonia by zero-valent iron, Chemosphere 35 (1997) 2689–2695.
[6] H. Huang, T.C. Zhang, Effects of low pH on nitrate reduction by iron powder, Water Res. 38 (2004) 2631–2642.
[7] M. Kumar, S. Chakraborty, Chemical denitrification of water by zero-valent magnesium powder, J. Hazard. Mater. B135 (2006) 112–121.
[8] S. Samatya, N. Kabay, U. Yuksel, M. Arda, M. Yuksel, Removal of nitrate from aqueous solution by nitrate selective ion exchange resins, React. Funct. Polym. 66 (2006) 1206–1214.
[9] J.J. Schoeman, A. Steyn, Nitrate removal with reverse osmosis in a rural area in South Africa, Desalination 155 (2003) 15–26.
[10] F. Hell, J. Lahnsteiner, H. Frischherz, G. Baumgartner, Experience with full-scale electrodialysis for nitrate and hardness removal, Desalination 117 (1998) 173–180.
[11] A. Pintar, J. Batista, J. Levec, Catalytic denitrification: Direct and indirect removal of nitrates from potable water, Catal. Today 66 (2001) 503–510.
[12] M.I.M. Soares, Biological denitrification of groundwater, Water Air Soil Pollut. 123 (2000) 183–193.
[13] K. Kaikake, Y. Baba, Highly selective adsorption resins, synthesis of chitosan derivatives and their adsorption properties for nitrate anion, Chem. Eur. J. 7 (1999) 471–472.
[14] N. Viswanathan, S. Meenakshi, Selective fluoride adsorption by a hydrotalcite/chitosan composite, J. Appl. Polym. Sci. 48 (2010) 607–611.
[15] C. Namasivayam, Removal and recovery of nitrate from water by $ZnCl_2$ activated carbon from coconut coir pith, an agricultural solid waste, Indian J. Chem. Technol. 12 (2005) 513–521.
[16] W.J. Huang, Y.L. Cheng, Effect of characteristics of activated carbon on removal of bromate, J. Sep. Sci. 59 (2008) 101–107.
[17] K.E. Perepelkin, N.V. Klyuchnikova, N.A. Kulikova, Experimental evaluation of man-made fibre brittleness, Chem. Fibers Int. 21 (1989) 1458–1466.

[18] M.S.A. Rahaman, A.F. Ismail, A. Mustafa, A review of heat treatment on polyacrylonitrile fiber, Polym. Degrad. Stab. 92 (2007) 1421–1432.
[19] Y.J. Bai, C.G. Wang, N. Lun, Y.X. Wang, M.J. Yu, B. Zhu, HRTEM microstructures of PAN precursor fibers, Carbon 44 (2006) 1773–1778.
[20] X. Chang, Q. Su, D. Liang, X. Wei, B. Wang, Efficiency and application of poly (acryldinitrophenylamidrazone dinitroacrylphenylhydrazin chelating fiber for pre-concentrating and separating trace Au(III), Ru(III), In(III), Bi(III), Zr(IV), V(V), Ga(III) and Ti(IV) from solution samples, Talanta 57 (2002) 253–261.
[21] S. Lee, K. Lee, S. Rhee, J. Park, Development of a new zero-valent iron zeolite material to reduce nitrate without ammonium release, J. Environ. Eng. 133 (2007) 6–12.
[22] K. Hristovski, A. Baumgardner, P. Westerhoff, Selecting metal oxide nanomaterials for arsenic removal in fixed bed columns: From nano powders to aggregated nanoparticle media, J. Hazard. Mater. 147 (2007) 265–274.
[23] Y. Wu, X. Wang, Preparation and characterization of single-phase α-Fe_2O_3 nano-powders by Pechini sol–gel method, Mater. Lett. 65 (2011) 2062–2065.
[24] W. Lin, Y. Lu, H. Zeng, Studies of the preparation, structure, and properties of an acrylic chelating fiber containing amidoxime groups, J. Appl. Polym. Sci 47 (1993) 45–52.
[25] Kh Saeed, S. Haidar, T.J. Oh, S. Park, Preparation of amidoxime-modified polyacrylonitrile (PAN-oxime) nanofibers and their applications to metal ions adsorption, J. Membr. Sci. 15 (2008) 400–405.
[26] L. Khezami, R. Capart, Removal of chromium (VI) from aqueous solution by activated carbons: Kinetic and equilibrium studies, J. Hazard. Mater. 123 (2005) 223–231.
[27] B.H. Hameed, A.A. Ahmad, N. Aziz, Isotherms, kinetics and thermodynamics of acid dye adsorption on activated palm ash, Chem. Eng. J. 133 (2007) 195–203.
[28] A.W. Adamson, A.P. Gast, Physical Chemistry of Surface. Inter Science Publisher, New York, NY, 1960.
[29] H. Zheng, Y. Wang, Y. Zheng, H. Zhang, H. Liang, M. Long, Equilibrium, kinetic and thermodynamic studies on the sorption of 4-hydroxyphenol on Cr-bentonite, Chem. Eng. J. 143 (2008) 117–123.
[30] H. Freundlich, Uber die adsorption in losungen (adsorption in solution), Z. Phys. Chem. 57 (1906) 384–470.
[31] M.M. Dubinin, E.D. Zaverina, L.V. Radushkevich, Sorption and structure of active carbons. I. Adsorption of organic vapors, Zh. Fiz. Khim. 21 (1947) 1351–1362.
[32] Y.S. Ho, G. McKay, Pseudo-second order model for sorption processes, Process Biochem. 34 (1999) 451–465.
[33] W.J. Weber, J.C. Morris, Kinetics of adsorption on carbon from solution, J. Sanit. Eng. Div. 89 (1963) 31–59.
[34] K.V. Kumar, V. Ramamurthi, S. Sivanesan, Modeling the mechanism involved during the sorption of methylene blue onto fly ash, J. Colloid Interface Sci. 284 (2005) 14–21.